

Dosimetry Evaluation of Treatment Planning Systems in Patient-Specific 3D Printed Anthropomorphic Phantom for Breast Cancer after Mastectomy using a Single-Beam 3D-CRT Technique for Megavoltage Electron Radiation Therapy

Endarko Endarko (PhD)^{1*}, Siti Aisyah (MSc)², Aditya Prayugo Hariyanto (MSc)¹, Mohammad Haekal (PhD)¹, Nandia Kavilani (BSc)², Ahmad Syafi'i (MSc)²

ABSTRACT

Background: The patient-specific 3D printed anthropomorphic phantom is used for breast cancer after mastectomy developed by the laboratory of medical physics and biophysics, Department of Physics, Institut Teknologi Sepuluh Nopember, Indonesia. This phantom is applied to simulate and measure the radiation interactions occurring in the human body either using the treatment planning system (TPS) or direct measurement with external beam therapy (EBT) 3 film.

Objective: This study aimed to provide dose measurements in the patient-specific 3D printed anthropomorphic phantom using a TPS and direct measurements using single-beam three-dimensional conformal radiation therapy (3DCRT) technique with electron energy of 6 MeV.

Material and Methods: In this experimental study, the patient-specific 3D printed anthropomorphic phantom was used for post-mastectomy radiation therapy. TPS on the phantom was conducted using a 3D-CRT technique with RayPlan 9A software. The single-beam radiation was delivered to the phantom with an angle perpendicular to the breast plane at 337.3° at 6 MeV with a total prescribed dose of 5000 cGy/25 fractions with 200 cGy per fraction.

Results: The doses at planning target volume (PTV) and right lung confirmed a non-significant difference both for TPS and direct measurement with *P*-values of 0.074 and 0.143, respectively. The dose at the spinal cord showed statistically significant differences with a *P*-value of 0.002. The result presented a similar skin dose value using either TPS or direct measurement.

Conclusion: The patient-specific 3D printed anthropomorphic phantom for breast cancer after mastectomy on the right side has good potential as an alternative to the evaluation of dosimetry for radiation therapy.

Citation: Endarko E, Aisyah S, Hariyanto AP, Haekal M, Kavilani N, Syafi'i A. Dosimetry Evaluation of Treatment Planning Systems in Patient-Specific 3D Printed Anthropomorphic Phantom for Breast Cancer after Mastectomy using a Single-Beam 3D-CRT Technique for Megavoltage Electron Radiation Therapy. *J Biomed Phys Eng.* 2023;13(3):217-226. doi: 10.31661/jbpe.v0i0.2111-1428.

Keywords

Electrons; Energy; Dosimetry; EBT3; Phantom; Radiation; Mastectomy; Three-Dimensional Therapy

Introduction

Frequent cancer in women is known as breast cancer, recorded from Globocan data in 2020 in Indonesia, i.e. breast cancer cases ranked at the top with a total of 65.858 cases out of a total of 396.914

¹Department of Physics, Institut Teknologi Sepuluh Nopember, Kampus ITS - Sukolilo Surabaya 60111, East Java, Indonesia

²Medical Physicist of Radiotherapy Installation, Naval Hospital Dr. Ramelan, Surabaya 60244, East Java, Indonesia

*Corresponding author: Endarko Endarko
Department of Physics, Institut Teknologi Sepuluh Nopember, Kampus ITS - Sukolilo Surabaya 60111, East Java, Indonesia
E-mail: endarko@gmail.com

Received: 8 November 2021
Accepted: 20 March 2022

other cancer cases [1]. In addition, based on the World Health Organization (WHO) data in 2018, breast cancer occupies the highest level of 16.7% of other cancer cases [2], reduced if cancer is treated with multidisciplinary treatments, including surgical treatment and radiation therapy. Radiation therapy can reduce the size and recurrence of local cancers [3]. Irradiation of the entire breast after mastectomy treatment is a standard method of controlling localized breast cancer recurrence. Radiotherapy after mastectomy as a breast cancer treatment strategy can reduce the risk of recurrence in the local area and breast cancer mortality [4].

A mastectomy is a form of early breast cancer treatment strategy by removing all the tissue in the breast area on the chest wall. In B Salvadori et al.s' study conducted based on a follow-up review for six years from the start of mastectomy treatment, a 35% risk of cancer recurrence was considered in patients treated with mastectomy without additional radiation therapy [5]. In addition, several studies on breast cancer provide further treatment in the form of radiation boosters, usually using electrons in the postoperative cancer area to increase local control in the breast area [6, 7].

Accordingly, an initial simulation process is needed before direct radiation to the patient. Cancer patients' initial simulation or treatment planning system must be simulated to calculate and optimize a patient's dose. Additionally, one of the cancer treatment planning technologies is 3D conformal radiation therapy (3D-CRT) [8], done using a three-dimensional volume-based charged particle radiation beam to achieve the suitability of the target volume area; the use of the beam's eye view can lead to a maximum and minimum the doses to the target and surrounding normal tissue, respectively. 3D-CRT technology is widely used to treat surface area breast cancer.

Radiation therapy for breast cancer covers various tissues with very different densities, such as bone, lung, soft tissue, air, and very

complex anatomy [9]. Meanwhile, some treatment planning systems (TPSs) have limitations for predicting low-density areas [9].

As an initial study on breast cancer individuals, an object similar to patients was needed in the medical world as a substitute called phantoms, used in quality control (QC) or quality tests on a linear accelerator (Linac) [10]. Therefore, dose measurements of the internal organs through detectors in phantoms will show the impact of the radiation interaction on the human being [9].

In this study, dosimetry of TPS was evaluated in a patient-specific 3D anthropomorphic phantom for breast cancer after mastectomy using a single-beam 3DCRT technique by electron radiation therapy, and the calibration of the EBT3 film was also conducted. Furthermore, the comparison doses from TPS and direct measurement using EBT3 film at planning target volume (PTV), right lung, spinal cord, and skin surface also are investigated.

Material and Methods

This experimental study was conducted at the Naval Hospital, Dr. Ramelan, Surabaya, and the data were Digital Imaging and Communications in Medicine (DICOM) from computed tomography (CT) (the GE Optima type) scan of the patient-specific 3D printed anthropomorphic phantom for post-mastectomy radiation therapy (PMRT) on the right side (see Figure 1) [11]. The phantom used was an in-house phantom (Registered Patent No. P00202102195) [11] developed by the Laboratory of Medical Physics and Biophysics, Department of Physics, Institut Teknologi Sepuluh Nopember, Surabaya, with length \times width \times height of $372.7 \times 265.7 \times 427$ mm³, respectively, and thickness of each slice was 1.5 cm.

1. Dosimeter Calibration of EBT3 film

Furthermore, the EBT3 film (Gafchromic, International Specialty Products, Wayne, NJ)

was used to measure the dose, and a calibration process was carried out on the EBT3 film according to the IAEA TRS protocol No. 398. The film sheet was cut according to the required dimensions and then placed right at the isocenter with a depth of 1.5 cm from the top surface of the 40×40 cm² water phantom slab (see Figure 2). The film was irradiated with an electron energy of 6 MeV and a dose variation from 100 to 700 cGy using Linac.



Figure 1: The patient-specific 3D printed anthropomorphic thorax phantom for post-mastectomy radiation therapy (PMRT).

Additional accessories were due to electron energy, namely an applicator 10×10 cm². The film sample was irradiated perpendicular to the electron source produced by Linac Elekta Precise at Naval Hospital. Dr. Ramelan, Surabaya. After the film was irradiated, it was scanned with EPSON Perfection V850 (Seiko Epson Corp., Nagano, Japan) and the software EPSON Scan V3.04. The scanned image was then analyzed using Image J software, and the pixel value was obtained by setting the region of interest (ROI). The pixel value obtained was converted into an average optical density value using the equation as follows [12]:

$$netOD = \log_{10} \left(\frac{P_{un}}{P_{ex}} \right) \quad (1)$$

where P_{un} is the selected pixel area value on the film without irradiation, and P_{ex} is the selected pixel area value after 6 MeV electron irradiation with various doses of 100-700 cGy [13, 14].

2. The single-beam 3D-CRT therapy plan

Radiation planning on the phantom was conducted using a 3D-CRT technique with the RayPlan 9A software. The phantom was irradiated with only one radiation field at a beam angle perpendicular to the breast plane at 337.3° and continued to set its energy at 6 MeV and a

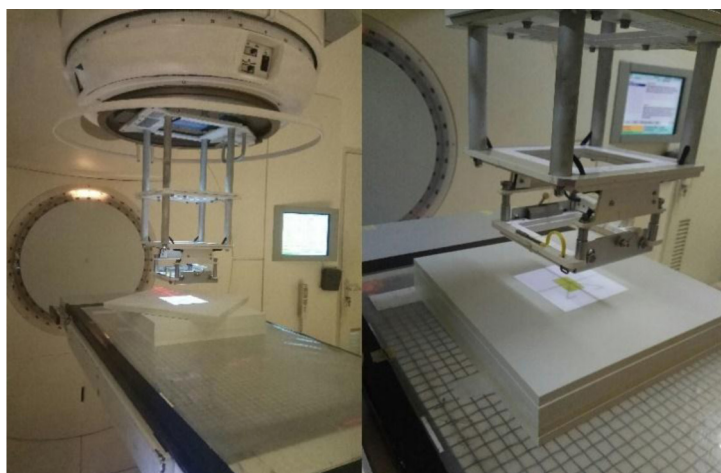


Figure 2: Experiment setup of dosimeter calibration of EBT3 film.

total prescribed dose of 5000 cGy/25 fractions per fraction of 200 cGy. After setting the clinical plan, the dose distribution was calculated, presented in the form of a dose-volume histogram (DVH), accordingly, the dose obtained for each organ at risk (OAR) and the planning target volume (PTV) were analyzed.

3. Dose Measurement Using EBT3 Film

The EBT3 film was cut according to the lungs, spine, and skin surface irradiation area. The irradiation technique onto the film was the same technique used in the TPS (see Figure 3), with the single-beam field of the 3DCRT technique, source axis distance (SAD) at 99.8 cm, energy 6 MeV, and 200 cGy/fraction with a

total prescribing dose of 5000 cGy, and a gantry angle of 337.3°. After irradiation, the film pieces were read using the EPSON Perfection V850 scanner (Seiko Epson Corp., Nagano, Japan) and the EPSON Scan V3.04 software. Furthermore, the image was processed with the ImageJ software; the reading result was a pixel area value used to obtain the NetOD value/optical density using equation (1) [14]. Moreover, the independent t-test was used to compare TPS doses and direct measurement doses for PTV, right lung, and spinal cord with a significance level of 5%.

Results

Figure 4 shows the results of calibration data of the EBT3 film presented in a dose curve as

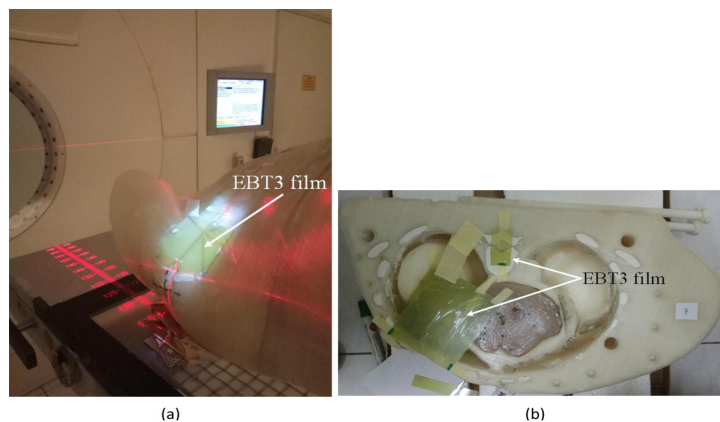


Figure 3: Setting-up of the EBT3 film onto patient-specific 3D printed anthropomorphic thorax phantom: (a) the surface of a phantom and (b) inside the phantom.

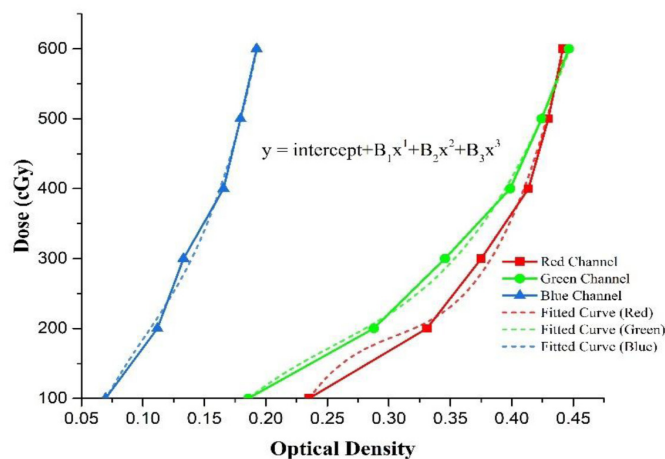


Figure 4: Dose as a function of optical density for EBT3 film calibration

a function of optical density. Meanwhile, the results of the fitting curve from Figure 4 for each red, green, and blue channel can be written as follows (2):

$$\begin{aligned}
 y_R &= -3460.9 + 34490.9x - 110716.7x^2 + 120880.3x^3 \\
 y_G &= -642.3 + 7748.4x - 26694.5x^2 + 34837.5x^3 \\
 y_B &= -316.4 + 9719.3x - 70147.9x^2 + 230148.4x^3
 \end{aligned}
 \tag{2}$$

where y_R (red channel), y_G (green channel), and y_B (blue channel) are the dose (cGy), and

x is the load input.

Furthermore, the effect of dose distribution governed by a single beam on treatment planning was that the isodose in the target area spreads with depth to the right lung organ adjacent to the PTV, as shown in Figure 5. Moreover, the other result of the TPS is the DVH statistical curve, as shown in Figure 6; based on the DVH curve, PTV (dark blue line) achieved an excess dose of the max-

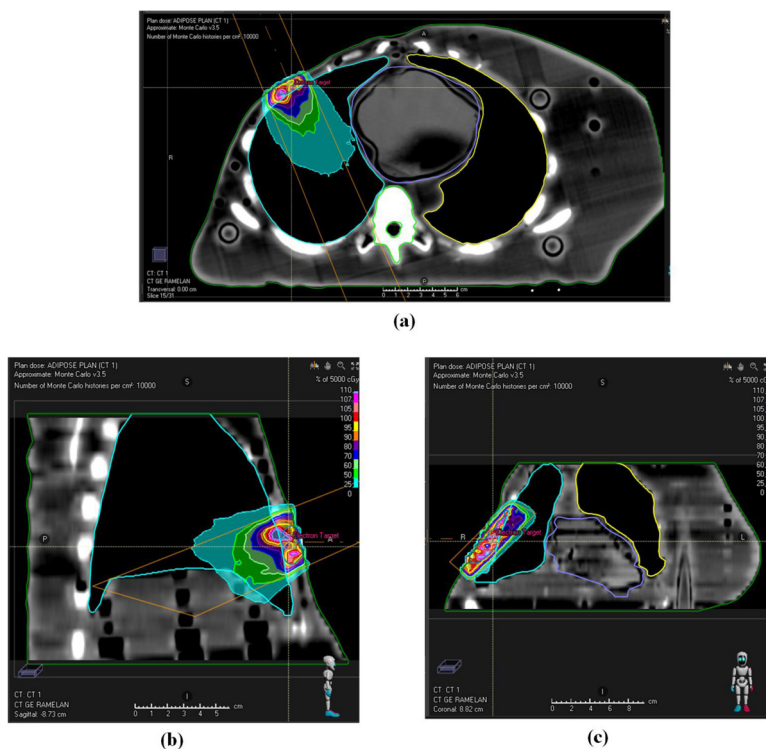


Figure 5: Simulation results of radiation treatment planning on the right chest area of the thorax phantom: a) axial, b) sagittal, and c) coronal.

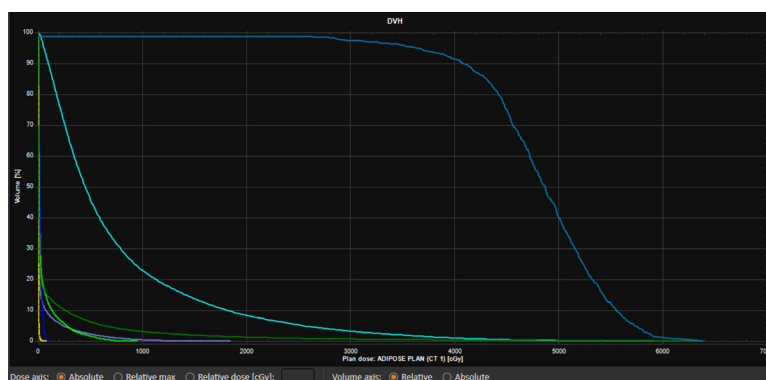


Figure 6: Dose-volume histogram (DVH) graph of treatment planning systems results of thorax phantom with an electron energy of 6 MeV.

imum (<107%).

Table 1 presents the absorbed dose of each organ based on the DVH curve in numerical form. DVH was calculated and generated using the TPS algorithm based on a three-dimensional object construction image [15].

Table 1 presents that for the PTV area, the maximum dose (D_1) is 6058 cGy, the minimum dose (D_{95}) is 3602 cGy, and the average dose ($D_{average}$) is 4758 cGy. In addition to PTV statistical data, other organs, such as the right lung, left lung respectively obtained an average dose of 740 and 4 cGy, with a limit of less than 1000-2000 cGy, and the heart dose was averaged 43 cGy with a limit of less than 2600 cGy; however, the maximum dose of the spinal cord was at 456 cGy with a limit (D_{max})=5000 cGy.

Meanwhile, the results obtained from direct dose measurements in phantom and TPS equipped with statistical analysis for differences in dose reading using an independent t-test are summarized in Table 2, showing the EBT3 film received absorbed doses on the chest wall, right lung, and spinal cord, 190, 138, and 3 cGy, respectively; however, TPS computed those doses 197, 129, and 5 cGy, respectively. Both measurements obtained a difference in dose readings of 7, 9, and 2 cGy. The difference in values in the chest wall and the right lung was still below the measurement difference limit of 10%. However, in the spinal cord, the difference in dose readings was more than 10% since the measured dose value was small in the spinal cord with a significant percentage difference.

Table 1: Absorbed dose results from treatment planning system with three-dimensional conformal radiation therapy (3DCRT) for energy at 6 MeV and dose of 50 Gy.

| Region of Interest (ROI) | ROI Volume (cm ³) | Total dose (cGy) | | | | | | |
|------------------------------|-------------------------------|------------------|----------|----------|---------------|----------|-------|-------|
| | | D_{99} | D_{98} | D_{95} | $D_{average}$ | D_{50} | D_2 | D_1 |
| Body | 9493.75 | 0 | 0 | 0 | 115 | 6 | 1409 | 2271 |
| Planning target volume (PTV) | 13.64 | 0 | 2904 | 3602 | 4758 | 4847 | 5967 | 6058 |
| Heart | 443.25 | 2 | 2 | 3 | 43 | 7 | 543 | 752 |
| Lung LF | 1098.34 | 0 | 1 | 2 | 4 | 4 | 12 | 16 |
| Lung RT | 1011.82 | 24 | 33 | 58 | 740 | 448 | 3438 | 3962 |
| Trachea | 7.58 | 7 | 7 | 8 | 21 | 18 | 64 | 70 |
| Spinal Cord | 202.10 | 5 | 5 | 6 | 48 | 10 | 456 | 562 |

LF: Left, RT: Right

Table 2: Comparison of results in dose measurements between treatment planning system (TPS) and direct measurement with the energy of 6 MeV and dose of 200 cGy.

| Organs at risk (OARs) | Measurement (cGy) | Treatment planning system (TPS) (cGy) | Difference (cGy) |
|--|-------------------|---------------------------------------|------------------|
| Chest wall (Planning target volume (PTV) area) | 190 | 197 | 7 ($P=0.074$) |
| Right lung | 138 | 129 | 9 ($P=0.143$) |
| Spinal cord | 3 | 5 | 2 ($P=0.002$) |
| Skin surface | 134 | 134 | 0 |

Discussion

Figure 4 shows each color channel with different sensitivity to the dose range as follows: 1) the red channel is sensitive at low dose rates up to a dose of 1000 cGy, 2) the green channel is sensitive at doses above 1000 cGy, and 3) the blue channel is sensitive at dose rates over 40 Gy or high dose rates [16]. This sensitivity curve can describe the maximum sensitivity for each color channel over the dose range [14]. Based on the sensitivity curve in Figure 4, the red channel has the highest sensitivity to low doses of 0-600 cGy than the green and blue channels. The red channel is the ideal color channel for reading low doses. When referring to the American Association of Physicists in Medicine (AAPM) TG-55 and 235 reports regarding GafChromic EBT3 films, the red channel is ideal for low dose measurements up to about 1000 cGy. However, the blue and green channels are less suitable at low doses, they are also suitable at doses above 1000 cGy [16].

The sensitivity of the film is also related to the frequency of the polychromatic light produced by the digitizer (film reader). The red channel obtained the reading results better than the green and blue channels when the film is irradiated with a 100-600 cGy. Several studies on EBT3 films, such as those conducted by Sorriaux J et al. for the energy of 6 MV photons and 6 MeV electrons, proved that the red channel is the most sensitive channel to low doses for the EBT3 film; however, the green channel is similar to the red channel with a dose range above 1000 cGy and for the blue channel had the lowest sensitivity compared to red and green channels [13]. León Marroquin et al. explained that the red channel was sensitive at a dose of 0-600 cGy, the green channel at 600-3500 cGy, and the blue channel at 3500-12000 cGy [14]. The sensitivity of the EBT3 film can be influenced by several factors, namely the method of scanning the film, exposure to visible light from the environment, film storage, treatment during scanning,

and the reading time. The reading time can give a dose difference greater than 10% if the film is scanned in the first 2 h after radiation and 3% within one day [17].

Planning with a single beam in TPS generally provides a dose with a distribution effect that continues to spread to depth. Therefore, the isodose in the target area continues to spread with depth to the right lung organ adjacent to the PTV as seen in Figure 5. However, as the penetrating power increases, the dose decreases. Although the dose distribution results spread out of the target field, the electron's energy still affects the OAR with low radiation. Electrons have lower penetrating power than photons [18].

Based on isodose color (as seen in Figure 5), green and blue colors dominate the lungs compared to other colors. The blue and green colors represent the percentage of doses received by the right lung of 25 and 50% of the total prescription dose of 5000 cGy. According to the dose distribution, as the depth of the dose spread increases, the dose decreases, as indicated by the color wash isodose formed. The average energy of electrons that pass through a material periodically decreases due to the interaction of Coulomb forces between the radiation beam and matter, and spread to the original path as its relatively low mass, the direction of travel can change easily during these interactions [6, 19]. Figure 5 also shows that the isodose does not cover the target with a maximum. The spread of isodose beyond the irradiation field boundary is due to the low energy beam producing a significant scattering and causing the isodose line to spread out of the irradiation field (Figure 5a). In addition, other factors with influenced the formation of isodoses are collimators, filter design (cerrobend), irradiation techniques, and irradiation angles [6].

Based on the DVH curve (Figure 6), it can be seen that PTV (thick dark blue line) obtained an excess dose of the maximum to be achieved, which is >107%. Due to inelastic

interactions with the coulomb field, bremsstrahlung tails are also formed on low-energy electrons [20]. The DVH curve for PTV is square, showing all prescribed doses cover 100% of PTV [21]. However, the results of the clinical are not always the same as the theory and also this plan. The shape of the DVH is influenced by the beam's interaction with the material before hitting the target volume and multileaf collimator (MLC) shape, which does not cover the entire target volume area so that some beams scatter off the field.

Cancer treatment plans optimize the treatment plans evaluated. Based on ICRU 50 and 62, the PTV area obtains a minimum dose coverage of 95% (4750 cGy) to 107% (5350 cGy) with 100% dose uniformity at PTV or $95\% \leq \text{PTV} \leq 107\%$ (4600-5000 cGy for whole breast/chest wall and node area). However, this study plan resulted in a dose at PTV exceeding 107% and less than 95%, i.e. the excess dose received by PTV was 708 cGy or (121%). The OAR closest to PTV was the right lung, which received an average of 740 cGy with a maximum of 3438 cGy. The lung threshold has a mean dose of less than 2000 cGy [22]. Furthermore, the heart received an average dose of 43 cGy and a maximum dose of 543 cGy. The heart must receive doses below 4000 cGy for the 100% volume threshold. Two organs (lungs and heart) are among the organs closest to the target. Radiation toxicity may occur if the lungs and heart receive a dose above the threshold. Therefore, all OARs in this plan obtained a safe dose.

The percentage difference in readings that is still below 10% (Table 2) is probably due to a slice shift between the position of the dose area in the TPS phantom image and the original phantom with the EBT3 films. When measuring directly, the electron beam is scattered in the air due to the interaction of electrons with the collimator and applicator so that the dose prescribed is not entirely on EBT3 films [23]. The spinal cord produces a high difference in readings because the dose read is very small.

In the current study, the difference between the dose measured and the TPS results are consistent with the study conducted by Stephen F. Kry et al. [23] which obtained a difference in skin dose measurements on average 22% or above 10% that was acceptable. All results from TPS and measurements with films resulted in doses that were still below tolerance despite the differences in the results obtained [23, 24]. The independent t-test for dose measurements between direct measurement and TPS for PTV and the right lung showed a non-significant difference with *P*-values of 0.074 and 0.143, respectively. In contrast, a significant difference was in the dose reading in the spinal cord with a *P*-value equal to 0.002.

Conclusion

The present study successfully demonstrated the planning treatment system for breast cancer radiation therapy using patient-specific 3D printed anthropomorphic phantom for breast cancer after mastectomy on the right side with the single beam 3DCRT technique.

The statistical analysis for dose measurement in PTV and right lung areas presented non-significant doses for both doses reading using TPS and direct measurement with EBT3 film. In contrast, dose reading in the spinal cord obtained a statistically significant difference. In addition, the use of the patient-specific 3D printed anthropomorphic phantom in quality control and radiation therapy quality assurance has promising clinical application opportunities.

Acknowledgment

The authors would like to thank the management of the Naval Hospital, Dr. Ramelan, Surabaya, Indonesia, for data collection and analysis at the Radiotherapy Facility.

Authors' Contribution

E. Endarko and S. Aisyah prepared and wrote the original draft. E. Endarko was involved in reviewing/editing the draft. E. Endarko, S.

Aisyah, AP. Hariyanto, and M. Haekal were involved in the investigation, samples preparation, methodology, data collection, and visualization. N. Kavilani and A. Syafi'i were involved in clinical planning, methodology, and data collection. All the authors read, modified, and approved the final version of the manuscript.

Ethical Approval

Naval Hospital Dr. Ramelan, Surabaya, Indonesia approved the protocol of the study.

Informed consent

The work was carried out on phantom and therefore, no participation consent was obtained.

Funding

This work was supported by the Institut Teknologi Sepuluh Nopember (ITS) and RISTEK-BRIN under Penelitian Dasar Unggulan Perguruan Tinggi (PDUPT) (No.966/PKS/ITS/2021).

Conflict of Interest

None

References

1. Globocan 2020. 360-indonesia-fact-sheets [Internet]. 2020 [cited 2021 October 1]. Available from: <https://gco.iarc.fr/today/data/factsheets/populations/360-indonesia-fact-sheets.pdf>.
2. WHO. Cancer Country Profile [Internet]. 2020 [cited 2021 October 1]. Available from: https://www.who.int/cancer/country-profiles/IDN_2020.pdf.
3. Harris JR. Fifty years of progress in radiation therapy for breast cancer. *Am Soc Clin Oncol Educ Book*. 2014;21-5. doi: 10.14694/EdBook_AM.2014.34.21. PubMed PMID: 24857056.
4. Suresh Moorthy PN, Saroj M, Hamdy EH. Dosimetric Characteristics of IMRT versus 3DCRT for Intact Breast Irradiation with Simultaneous Integrated Boost. *Austral-Asian Journal of Cancer*. 2012;11(3):10.
5. Salvadori B, Marubini E, Miceli R, Conti AR, Cusumano F, Andreola S, Zucali R, Veronesi U. Reoperation for locally recurrent breast cancer in patients previously treated with conservative surgery. *Br J Surg*. 1999;86(1):84-7. doi: 10.1046/j.1365-2168.1999.00961.x. PubMed PMID: 10027366.
6. Khan FM, Gibbons JP. Khan's the physics of radiation therapy. Lippincott Williams & Wilkins; 2019.
7. Wilkens JJ. Introduction to Radiotherapy with Photon and Electron Beams and Treatment Planning from Conformal Radiotherapy to IMRT. *AIP Conference Proceedings*. 2007;958(1):63-9. doi: 10.1063/1.2825834.
8. Prior P, Sparks I, Wilson JF, Bovi J, Currey A, Bradley J, et al. Use of Three Dimensional Conformal Radiation Therapy for Node Positive Breast Cancer Does Not Result in Excess Lung and Heart Irradiation. *International Journal of Medical Physics, Clinical Engineering and Radiation Oncology*. 2017;6(1):1-9. doi: 10.4236/ijmpcero.2017.61001.
9. Pimenta EB, Nogueira LB, de Campos TPR. Dose measurements in a thorax phantom at 3DCRT breast radiation therapy. *Rep Pract Oncol Radiother*. 2021;26(2):242-50. doi: 10.5603/RPOR.a2021.0037. PubMed PMID: 34211775. PubMed PMID: PMC8241292.
10. Behmadi M, Gholamhosseinian H, Mohammadi M, Naseri S, Momennezhad M, Bayani S, Bahreyni Toossi MT. Evaluation of Breast Cancer Radiation Therapy Techniques in Outfield Organs of Rando Phantom with Thermoluminescence Dosimeter. *J Biomed Phys Eng*. 2019;9(2):179-188. doi: 10.31661/JPPE.V010.1067. PubMed PMID: 31214523. PubMed PMID: PMC6538909.
11. Endarko E, Hariyanto AP. 3D Fantom Antropomorfik Untuk Jaminan Kualitas Radioterapi Pada Kasus Kanker Payudara Pasca-Mastektomi. Patent: P00202102195. Indonesia; 2021.
12. Sipilä P, Ojala J, Kajaluoto S, Jokelainen I, Kosunen A. Gafchromic EBT3 film dosimetry in electron beams - energy dependence and improved film read-out. *J Appl Clin Med Phys*. 2016;17(1):360-73. doi: 10.1120/jacmp.v17i1.5970. PubMed PMID: 26894368. PubMed PMID: PMC5690204.
13. Sorriaux J, Kacperek A, Rossomme S, Lee JA, Bertrand D, Vynckier S, Sterpin E. Evaluation of Gafchromic® EBT3 films characteristics in therapy photon, electron and proton beams. *Phys Med*. 2013;29(6):599-606. doi: 10.1016/j.ejmp.2012.10.001. PubMed PMID: 23107430.
14. Marroquin EY, Herrera González JA, Camacho López MA, Barajas JE, García-Garduño OA. Evaluation of the uncertainty in an EBT3 film dosimetry system utilizing net optical density. *J Appl Clin Med Phys*. 2016;17(5):466-81. doi: 10.1120/jacmp.v17i5.6262. PubMed PMID: 27685125. PubMed PMID: PMC5874103.
15. Lee S, Cao YJ, Kim CY. Physical and radiobiologi-

- cal evaluation of radiotherapy treatment plan. In: Nenoj M., editors. Evolution of ionizing radiation research. Rijeka, Croatia: InTech; 2015. p. 109-50.
16. Niroomand-Rad A, Chiu-Tsao ST, Grams MP, Lewis DF, Soares CG, et al. Report of AAPM Task Group 235 Radiochromic Film Dosimetry: An Update to TG-55. *Med Phys*. 2020;**47**(12):5986-6025. doi: 10.1002/mp.14497. PubMed PMID: 32990328.
 17. Howard ME, Herman MG, Grams MP. Methodology for radiochromic film analysis using FilmQA Pro and ImageJ. *PLoS One*. 2020;**15**(5):e0233562. doi: 10.1371/journal.pone.0233562. PubMed PMID: 32437474. PubMed PMCID: PMC7241712.
 18. Park SH, Kim JC. Comparison of electron and x-ray beams for tumor bed boost irradiation in breast-conserving treatment. *J Breast Cancer*. 2013;**16**(3):300-7. doi: 10.4048/jbc.2013.16.3.300. PubMed PMID: 24155759. PubMed PMCID: PMC3800726.
 19. Gerbi BJ, Kirova YM, Orecchia R. Clinical Applications of High-Energy Electrons. Levitt SH, Purdy JA, Perez CA, Poortmans P., editors. Technical Basis of Radiation Therapy. New York: Springer; 2006. p. 135-65.
 20. Mott JHL, West NS. Essentials of Depth Dose Calculations for Clinical Oncologists. *Clin Oncol (R Coll Radiol)*. 2021;**33**(1):5-11. doi: 10.1016/j.clon.2020.06.021. PubMed PMID: 32718763.
 21. Stewart AJ, O'Farrell DA, Cormack RA, Hansen JL, Khan AJ, Mutyala S, Devlin PM. Dose volume histogram analysis of normal structures associated with accelerated partial breast irradiation delivered by high dose rate brachytherapy and comparison with whole breast external beam radiotherapy fields. *Radiat Oncol*. 2008;**3**:39. doi: 10.1186/1748-717X-3-39. PubMed PMID: 19019216. PubMed PMCID: PMC2612673.
 22. Marks LB, Yorke ED, Jackson A, Ten Haken RK, Constine LS, et al. Use of normal tissue complication probability models in the clinic. *Int J Radiat Oncol Biol Phys*. 2010;**76**(3 Suppl):S10-9. doi: 10.1016/j.ijrobp.2009.07.1754. PubMed PMID: 20171502. PubMed PMCID: PMC4041542.
 23. Kry SF, Smith SA, Weathers R, Stovall M. Skin dose during radiotherapy: a summary and general estimation technique. *J Appl Clin Med Phys*. 2012;**13**(3):3734. doi: 10.1120/jacmp.v13i3.3734. PubMed PMID: 22584171. PubMed PMCID: PMC5716567.
 24. Bauk S, Alam MS, Alzoubi AS. Precision of Low-Dose Response of LiF:Mg, Ti Dosimeters Exposed to 80 kVp X-Rays. *J Phys Sci*. 2011;**22**(1):125-30.